Mechanism of groundwater inrush hazard caused by solution mining in a multilayered rock salt mining area: A case study from Tongbai County, China

Bin Zeng[1*], Tingting Shi[2], Zhihua Chen[1], Liu Xiang[3], Shaopeng Xiang[4], Muyi Yang[1]

[1]. School of Environmental Studies, China University of Geosciences, Wuhan 430074, Hubei, P.R.China.

[2]. Three Gorges Research Center for Geo-Hazard, Ministry of Education, Wuhan 430074, Hubei, P.R.China.

[3]. Department of Geological Engineering, Hubei Land Resources Vocational College. Wuhan 430074, P.R.China.

[4]. Hydrological Engineering Environment Technology Consulting Co. Ltd. Wuhan 430074, P.R.China.

****Corresponding author***: Bin Zeng, Ph.D.

Affiliation: School of Environmental Studies, China University of Geosciences.

Affiliation address: No. 388 Lumo Road, Wuhan, Hubei, 430074, P.R. China.

Email: zengbin_19@126.com. Tel: 86-27-67883473. Fax: 86-27-87436235.

ABSTRACT

The solution mining of salt mineral resources may contaminate groundwater and lead to water inrush out of the ground due to brine leakage. Taking a serious groundwater inrush hazard in a large salt mining area in Tongbai County, China, as an example, this study mainly aims to analyse the source and channel of the inrushing water. The mining area has three different types of ore beds as follows: a) trona (trisodium hydrogendicarbonate dihydrate, also sodium sesquicarbonate dihydrate, with the formula Na_2CO_3•$NaHCO_3$•$2H_2O$, is a non-marine evaporite mineral); b) glauber (sodium sulphate is the inorganic compound with the formula Na_2SO_4 as well as several related hydrates) and c) gypsum (a soft sulphate mineral composed of calcium sulphate dihydrate, with the chemical formula $CaSO_4 \cdot 2H_2O$). Based on the understanding of geological and hydrogeological conditions, the study first obtained hydrochemical data of the groundwater at different points and depths, and then analysed the pollution source and pollutant component from single or mixed brines using both physical-chemical reaction principle analysis and a hydrogeochemical simulation method. Finally possible leakage brine conducting channel to the ground was discussed from both geological and artificial aspects. The results reveal that the brine from the trona mine is the major pollution source; there is a fissure zone in the NW-SE direction controlled by the geological structure that provides the main channels for the leakage brine to flow into the aquifer around the water inrush regions, and a large number of waste gypsum exploration boreholes are the channels that supply the polluted groundwater inrush out of the ground. This research can offer a valuable reference for avoiding and assessing groundwater inrush hazards in similar rock salt mining areas, which is advantageous for both groundwater quality protection and public health.

1. **Introduction**

Solution mining is commonly used in salt mine exploitation, as salts are soluble in water. In this method, high-pressure and -temperature water with low salinity is injected into a mineral deposit through production wells to dissolve the mineral salts. After being drawn from the wells, the soluble salt is purified and further processed. However, the high-pressure and -temperature water used in this process not only dissolves minerals but can also cause fracturs in the strata, which usually results in hazards such as brine leakage or groundwater inrush. In this situation underground drinking water for the public is normally polluted following groundwater inrush, creating a hazard and threatening the health of local residents.

Many scholars (Clark and Fritz, 1997; Liu et al., 2015; Wu et al., 2016) have studied groundwater inrush hazards in both coal and metal mines, and some adopted methods are as follows: the use of water level / temperature criterion (Yuan and Gui, 2005; Ma and Qian, 2014), stochastic simulation (Fernandez-Galvez et al., 2007), numerical simulation (Liu et al., 2009; Kang et al., 2012; Shao et al., 2013; Houben, et al., 2017), water chemical analysis (isotope analysis, water quality type correlation analysis) (Robins, 2002; Fernandez et al., 2005; Hu et al., 2010; Cobbina et al., 2015; Lee et al., 2016; LeDoux et al., 2016), multivariate statistics (discriminant analysis, clustering analysis) (Chen and Li, 2009; Lu, 2012) , fractional advection dispersion equations (Ramadas et al., 2015) and nonlinear analysis (fuzzy mathematics, grey correlation analysis, etc.) (Hao et al., 2010; Gao, 2012). However, due to the particularity of the solution mining method and the complex chemical-physical reactions during the high-pressure and -temperature mining process, research regarding solution mining was more focused on mining techniques (Jiang and Jiang, 2004; Kotwica, 2008; Namin et al., 2009), mining cavity stability analysis and sinkhole problems (Staudtmeister and Rokahr, 1997; Bonetto et al., 2008; Ezersky et al., 2009; Goldscheider and Bechtel, 2009; Closson and Abou Karaki, 2009; Vigna et al., 2010; Frumkin et al., 2011; Ezersky and Frumkin, 2013; Qiu, 2011; Blachowski et al., 2014), and geohazards particularly in karst areas due to human-induced underground caving (Waltham and Fookes 2003; Parise and Gunn 2007; Zhou and Beck 2011; Parise and Lollino 2011; Lollino et al., 2013; Gutierrez et al., 2014; Parise et al., 2015), but rarely on source and channel analysis of inrush water in a solution mining accident.

The studied rock salt mining area is in Tongbai County, Henan Province, China. This mining area has the second largest trona reserves in the world, while its glauber salt reserves reach 45 million tons. Since trona and glauber salt were put into production in 1990 with single- and double-well convection mining as the main producing method, five inrush points appeared in the town of Anpeng, Tongbai County, from June 2011 to May 2013. Among these five inrush points, four (Y1~Y4) were long-term (longer than 2 years) with stable discharge, while one (Y-5) was a sudden inrush point (as shown in Fig. 1 and Fig. 2). On 1 February 2013, almost 200 m^3 of mud and sediment erupted out of the ground at the Y-5 point. The area of the inrush point was almost 4 m^2; the average water inflow was from 20-30 m^3/d

while the greatest inflow reached 200 m^3/d. The water inrush lasted for approximately three months. During the Y-5 inrush accident, according to the field investigation, a trona production well named “S02,” which is 200 m from the inrush point, broke at a depth of 234 m and remained broken for a long period of time. It was repaired on 15 March 2013. During the entire water inrush process, the inrush of groundwater led to a phenomenon of salinization at the base of the houses of many villagers, and made water in many residents’ wells no longer drinkable.

Since the groundwater inrush hazard involved a wide geographic area and the inrush source was quite hard to distinguish due to the multi-layer distribution of the different ore bodies and the complexity of the inrush water component. Therefore, in order to put forward a targeted treatment program to stop the water inrush as soon as is possible, and mitigate the groundwater pollution in research region, the source and channel of the inrush water were taken as the research emphasis in this study. Furthermore, this research can provide a valuable reference for avoiding and assessing groundwater inrush hazards in similar rock salt mining areas, which is advantageous for both groundwater quality protection and public health.

2. Geological and hydrogeological setting

2.1. Geological conditions

The mining area is located northwestern Tongbai County. The landscape is characterised by hollows and ridges, and has an elevation ranging from 140 to 200 m. The strata, lithology, aquifer, and the position of different ore beds in the research area (Shi et al., 2013) are shown in Fig. 3.

According to geologic references and field investigation, in the northeastern mining area, a hidden east-west oriented fault is developed at the bottom of the first segment of the Hetaoyuan Formation, and another four, hidden, south-north oriented faults are developed at the bottom of the second segment of the Hetaoyuan Formation. These five faults are outside the scope of trona mine, so they have had little effect on the ore bed. A few small-scale hidden faults are developed at the bottom of the third segment of the Hetaoyuan Formation, although within the scope of the glauber salt mine, they have had little effect on the glauber salt ore bed which is distributed at the top of the first segment of Hetaoyuan Formation, A hidden east-west oriented fault is developed at the bottom of the Liaozhuang Formation in the range of the glauber salt mine, but it has had little effect on the glauber salt mine because of its small scale.

2.2. Hydrogeological conditions

The groundwater in the mining area can be divided into pore water in the loose rock mass and bedrock fissure water according to the lithology and hydrogeological features. In the upper part of the Liaozhuang Formation, a mudstone interbedded with gypsum is considered a relative weak permeable stratum especially under the condition of high-pressure and -temperature water injection during the mining period. The shallow aquifer is unconsolidated pore water above this weak permeable stratum, while the deep aquifer is a bedrock fissure beneath this weak permeable stratum.

The flow direction of the shallow groundwater is controlled by the overall terrain. Taking the underground watershed as the boundary, the groundwater on the south side of the watershed is mainly flowing from northeast to southwest with the Yanhong River as the base of the drainage, while the groundwater on the north side of the watershed is mainly slowing from south to north with the Xia River as the base of the drainage. The deep groundwater has relatively closed burial conditions, slow velocity, and nearly the same flowing direction as the shallow groundwater. The water inflow of a single well with poor water content is approximately 100 m^3/d, while it can reach from 1000-2000 m^3/d if it has rich water content. The annual variation of the groundwater level is from 2-4 m, while the depth is stable at 2.3-4 m. Residents in Anpeng use groundwater as the source of their drinking water, which comes from wells and is from the porous aquifer.

As shown in Fig. 3, gypsum mainly occurs on the top of the Liaozhuang Formation, glauber salt occurs in the third member of the Hetaoyuan Formation, and the trona occurs at the bottom of the second member of the Hetaoyuan Formation as well as on top of the first member of the Hetaoyuan Formation. The surrounding rocks of every mineral layer include mudstone, shale, sandy conglomerate, psammitic rock and dolomite, which have sufficient thickness and good water-resistance. Therefore, the effect of groundwater on the mineral deposit is minimal in the mining area.

2.3 Distribution and characteristics of the ore body

The three ore bodies overlap in plane distribution, as shown in Fig. 4. The vertical distribution of the ore bodies from deep-to-shallow is trona (buried depth: 1560.92-2929.53 m), glauber salt (buried depth: 1003.66-1397.58 m) and gypsum (buried depth: 134-338 m). The trona and glauber salt bodies are at least 250 m apart from each other vertically.

The trona has 11 horizontal layers, with an average thickness of 2.11 m. The chemical composition of trona is mainly $NaHCO_3$ (average of 77.06%) and Na_2CO_3 (average of 16.33%) (Wang, 1987). The glauber salt has 4 layers, with an average thickness of 8.93 m. The dip angle of the ore bed layer is less than 10°. The average mineral grade is 60.14%. The main composition of the glauber salt is Na_2SO_4 (>90%) with a small amount of NaCl.

3. Methods

Based on the field investigation results, the chemical characteristic analysis of the inrush water at different sites and time, analysis of the physical and chemical reaction principles for the different brines, and combined with the PHREEQC simulation method the source of the inrush water was determined.

3.1. Sampling and testing

The five groundwater inrush points (Y1~Y5) and some shallow groundwater points (resident wells: SY1~SY6) near the accident site were chosen as groundwater quality sampling points, as shown in Fig. 4. Water from each point was sampled on 9 March 2013.

Water samples were filtered using a 0.45 μm millipore filtration membrane in the field, and then filled with a polyethylene bottle which had been soaked in acid and washed with deionised water. Filtered water samples were acidified until the pH<2 by addition of ultra-pure HNO_3^- for the determination of cations; water samples for the determination of anions were not treated.

Elements tested in the laboratory included 26 cations (K^+, Na^+, Ca^{2+}, Mg^{2+}, Sr^{2+}, etc.) and 5 anions (F^-, Cl^-, NO_3^-, SO_4^{2-}, NO_2^-). The instrument used for the determination of cations was an inductively coupled plasma atomic emission spectrometer (Agilent ICP-OES 5100), and the minimum detection limit was 0.0001mg/L. The instrument used for the determination of anions was an ion chromatograph (ICS-1100), and the minimum detection limit was 0.001 mg/L. CO_3^{2-} and HCO_3^- were tested according to the "Groundwater quality test method: Determination of carbonate and bicarbonate by hydroxide titration (DZ/T 0064.49-93)," and the minimum detection limit was 0.01 mg/L.

In addition, from March to April 2013, at the Y-5 and Y-3 points, three water quality automatic recorders (Levelogger gold, Canada) were arranged for inrush water monitoring. Monitoring indicators were temperature, water level and electrical conductivity. The purpose of the monitoring was to fully understand the inrush water quality during the whole accident, especially in the process of well reparation.

3.2. Analysis of the physical and chemical reaction principles in different brine mixing conditions

During the accident, the leakage brine of the trona (2000 m belowground) or glauber salt (1000 m belowground) might flow through the gypsum deposit (200-400 m belowground), which is comprised primarily of $CaSO_4$, and cause physical and chemical reactions while it inrushes out of the ground. Thus, the formation of the inrush water chemistry component might be from glauber brine, or trona brine, or a mixture of the two brines, flowing through the gypsum layer with accompanying physical and chemical reactions. To provide the basis for further analysis of the inrush water source, the physical solubility of the gypsum and the reaction when the glauber salt brine, trona brine, or a mixture of trona and glauber salt brine flowing through the gypsum deposits were analysed.

3.2.1. The physical solubility of gypsum ($CaSO_4$)

Gypsum is slightly soluble; when in water, its acidity is apparent. Eq. (1) provides the dissolution rate equation of gypsum in water:

$$R_{Gypsum} = k_1 \times \frac{\mathrm{A}_g}{V}\left(1 - \left(\frac{IAP}{K}\right)_{Gypsum}\right) \tag{1}$$

R_{Gypsum}: the dissolution rate of gypsum; k_1: rate constant; A_g: the surface area of gypsum; V: the liquid volume in contact with the gypsum surface; IAP: the product of ion activity; and K: ion solubility product.

$\left(\frac{IAP}{K}\right)_{Gypsum}$ is affected by the temperature; thus, it is the same as R_{Gypsun}.

The solubility of gypsum in water reaches a maximum of 0.2097 g/100 g at 40℃. The solubility decreases when the temperature is below or above 40℃. The content of SO_4^{2-} and Ca^{2+} obtained by physical dissolution is very low.

3.2.2. Gypsum ($CaSO_4$) dissolved by glauber salt brine (Na_2SO_4)

Equations (2) and (3) show the reactions of Na_2SO_4 and $CaSO_4$ with water.

$$Na_2SO_4 \leftrightharpoons 2Na^{+} + SO_4^{2-} \quad (2)$$

$$CaSO_4 \leftrightharpoons Ca^{2+} + SO_4^{2-} \quad (3)$$

Because of the common-ion effect, the solubility of the electrolyte will decrease when a strong electrolyte with the same ion is placed into an electrolyte-saturated solution. Thus, the solubility of gypsum will be reduced when glauber salt brine flows through and dissolves the gypsum deposits; the gypsum will be even harder to dissolve in this situation. Thus, if the glauber salt brine flows through the gypsum deposits, the brine characteristic would not apparently change.

3.2.3. The reaction of trona brine or a mixture of trona and glauber salt brine with gypsum

The HCO_3^- and CO_3^{2-} contents in trona brine or in mixed brine are very high as is the solution alkalinity and pH. If the reaction kinetics is not taken into account, the pH has little influence on the dissolution of gypsum (Yang, 2003; Xu and Li, 2011). The reaction occurs when the brine with high concentrations of HCO_3^- and CO_3^{2-} flows through the gypsum deposits. The main chemical reactions are as follows:

$$Na_2CO_3+CaSO_4 \leftrightharpoons Na_2SO_4+CaCO_3\downarrow \quad (4)$$

$$2NaHCO_3+CaSO_4 \leftrightharpoons Ca(OH)_2+ Na_2SO_4+2CO_2\uparrow \quad (5)$$

In Eq. (4), $CaSO_4$ is slightly soluble, while $CaCO_3$ is insoluble. The reaction easily occurs when an insoluble substance is produced by a slight soluble substance, and the ionic equation is as follows:

$$CO_3^{2-}+CaSO_4 \cdot 2H_2O \leftrightharpoons SO_4^{2-}+CaCO_3\downarrow+2H_2O \quad (6)$$

The Gibbs Free Energy (ΔG) is -22.7 kJ/mol under the standard state. When ΔG is negative, the reaction, which is endothermic, occurs freely. The reaction is faster at higher temperatures. Eq. (5) shows that ΔG is 2102 kJ/mol under the standard state. When ΔG is positive, the reaction will not freely occur.

Thus, the reaction shown in Eq. (5) will not occur, but the chemical reaction will still proceed as shown in Eq. (4), when trona brine or mixed brine flow through the gypsum deposits.

3.2.4. The carbonate equilibrium effect during the reaction of different brines

The carbonate equilibrium that exists in the trona brine or mixed brine is affected by pH. The carbonate in groundwater exists in three forms: free carbonic acid, bicarbonate and carbonic acid.

In the trona brine (pH>10), the concentration of HCO_3^- is 5-20 times that of the concentration of CO_3^{2-}, and CO_3^{2-} in the brine is dominant in this case. When the trona brine flows through the gypsum, $CaSO_4$ reacts with CO_3^{2-} and $CaCO_3$ precipitates. If the concentration of CO_3^{2-} in the brine decreases, a reversible reaction will take place and drive the equilibrium to the right. Thus, the reverse reaction will occur when the trona brine flows through the gypsum as follows:

$$CO_3^{2-}+CaSO_4 \leftrightharpoons SO_4^{2-}+CaCO_3\downarrow \tag{7}$$

$$HCO_3^{-} \leftrightharpoons H^{+}+CO_3^{2-} \tag{8}$$

The circular reactions as shown in Eqs. (7) and (8) will occur when mixed brine flows through the gypsum because it has similar properties to the trona brine. Thus, taking the carbonate equilibrium effect into account, the concentrations of HCO_3^- and CO_3^{2-} will decrease, while SO_4^{2-} increases after $CaCO_3$ precipitates.

3.3. Simulation of groundwater inrush source

For further quantitative analysis of the inrush water source and component, the international hydrological and geochemical simulation software PHREEQC was used to simulate the water-rock interaction. The PHREEQC (D.L. Parkurst and C.A.J. Appelo, 1999) software was developed by the U.S. Geological Survey, and it is able to calculate geochemical action within a temperature range of from 0~300 degrees (Wei, 2010).

Based on the deduction that the main water inrush source around Anpeng was trona leakage brine, the simulation method PHREEQC was used and combined with the possible channel of inrush water to establish a conceptual model and then hydrogeochemical simulation of the water-rock interaction was conducted. Subsequently, the mixed ratio of inrush groundwater and shallow groundwater around Anpeng were quantified, which can better verify the source of the inrush water.

3.3.1. Conceptual model

Around Anpeng, the trona leakage brine flowed through the specified mineral assemblages and mixed with shallow groundwater in different proportions.

3.3.2. Initial data input

The parameters of the trona brine were taken from the enterprise's production testing data; the parameters of the shallow groundwater were taken from the same aquifer but outside the study area, and can basically represent groundwater background values. The specific parameters are shown in Table 1.

3.3.3. Setting of stratum and mineral

The formations from the bottom to the top during the process of the leakage brine flowing into the shallow groundwater and then flowing out of the ground were as follows: the third member of the Hetaoyuan Formation of Paleogene, and the Liaozhuang Formation and Fenghuang Formation of Neogene and Quaternary, respectively. To simplify the mining area, according to the thickness of the rock stratum and the proportion of mineral composition，it can be assumed that the layer through which the trona brine flowed contains Ca-montmorillonite, kaolinite, gypsum, potash feldspar and potash mica.

The main ingredients are as follows: Kaolinite: $Al_4[Si_4O_{10}](OH)_8$; Gypsum: $CaSO_4 \cdot 2H_2O$; Ca-montmorillonite: $(Na,Ca)_{0.33}(Al,Mg)_2[Si_4O_{10}](OH)_2 \cdot nH_2O$; Dolomite: $CaCO_3$; Potash feldspar: K

[$AlSi_3O_8$]; Potash mica: aluminium silicate as K, Al, Mg, Fe and Li.

4. Results and Discussion

On 9 March 2013, in Anpeng, water samples from five groundwater inrush points and six surrounding water quality monitoring points (resident well) were tested. The results of water chemical composition are shown in Table 2, and the distribution of the sampling points is shown in Fig. 4.

According to the water quality analysis, the inrush brine had a relatively high salinity, with some inrush water samples containing SO_4-Na and some containing HCO_3-Na. The crystals mainly consisted of $NaSO_4$, Na_2CO_3, and $NaHCO_3$. The composition of the inrush water and the crystals was the same as that of the high-concentrated ions in the trona brine (Na_2CO_3, $NaHCO_3$, etc.) and glauber salt brine (Na_2SO_4).

4.1. The source of the inrush water

An automatic water quality recorder was set up at the Y5 inrush point on 4 March 2013. The monitoring lasted from 5 March to 20 March 2013. Thus, the relationship between the inrush points and the S02 well can be assessed according to the correlation of the changes between temperature/electrical conductivity and the concentration of brine during the S02 production well reparation period (5 March to 14 March 2013).

The production of glauber ceased during the investigation (2 March to 15 March 2013), so it could be determined how the glauber mining affects the water inrush hazard based on a dynamic water quality situation.

4.1.1. The source of inrush water at the Y-5 point

After successful reparation of the S02 well, the conductivity and temperature of the inrush water decreased significantly. The CO_3^{2-} concentration remained at 0, the concentration of HCO_3^- decreased to 500 meq/L, while the concentration of SO_4^{2-} increased to 600 meq/L. Subsequently, the concentrations of these three ions were in a state of dynamic balance. The analysis shows that the source of the inrush water at the Y-5 point is closely related to the S02 trona well.

In order to ensure whether the glauber brine exists at this point as part of an inrush source, further analysis was performed. The depth of the well rupture was 234 m; the gypsum deposit was developed to this depth. While the leakage of the trona brine flowed through the gypsum deposit, reactions would occur as shown in Eqs. (7) and (8).

According to the ion milliequivalent concentrations (Ca^{2+} 0.61 meq/L; CO_3^{2-} 905.3 meq/L; HCO_3^- 1332.94 meq/L; Cl^- 107.43 meq/L; and SO_4^{2-} 267.89 meq/L) at the Y-5 point, the concentration of Ca^{2+} was negligible compared to the other main ions. Only the reaction between CO_3^{2-} and $CaSO_4$ had to be taken into account because of the large number of CO_3^{2-}, fast velocity, the short contact time with gypsum, and the high temperature. The reaction of CO_3^{2-} and $CaSO_4$ would take place at a ratio of 1:1 according to Eq. (7), and three types of inrush water sources could be assumed under this precondition as follows:

(1) The inrush water source was only from the trona brine.

The CO_3^{2-} and $CaSO_4$ in the brine reacted at a ratio of 1:1, and the concentration of SO_4^{2-} was equal to the reacted γCO_3^{2-} content. Thus, the $\gamma CO_3^{2-}/\gamma HCO_3^-$ ratio in the trona brine was equal to the $\gamma(CO_3^{2-}+SO_4^{2-})/\gamma HCO_3^-$ ratio in the inrush water. From this calculation, it could be seen that $\gamma(CO_3^{2-}+SO_4^{2-})/\gamma HCO_3^-$ was equal to 0.88, while $\gamma CO_3^{2-}/\gamma HCO_3^-$ ranged between 0.86 and 1.26. The content of $\gamma(CO_3^{2-}+SO_4^{2-})/\gamma HCO_3^-$ was similar to $\gamma CO_3^{2-}/\gamma HCO_3^-$; therefore, the source of the inrush water was exclusively trona brine.

(2) The inrush water source was only from the glauber brine.

The $\gamma SO_4^{2-}/\gamma HCO_3^-$ ratio in the glauber brine was equal to 1237.8, compared to 0.19 in the inrush water. Therefore, this assumption was incorrect because of the widely varying ratios.

(3) The inrush water source was from a mixed brine of glauber and trona,

Assuming that the contribution ratio of the glauber brine was X and that of the trona brine was Y was true, then $1237.8 \times X + (0.86{\sim}1.26) \times Y = 0.88$. This equation showed that when the contribution ratio of the trona brine was equal to 1, the contribution ratio of the glauber brine was equal to 1.6×10^{-5} and was too small to ignore.

Thus, it could be confirmed that the water inrush source at Y-5 was exclusively the leakage of trona brine from the broken S02 well.

4.1.2. The sources of inrush water at the Y-4, Y-3, Y-2, and Y-1 points

The inrush water quantity and the dynamic variation of the concentration of SO_4^{2-} and HCO_3^- at points Y1-Y4 were not obvious when the S02 well was under repair and all the glauber wells were shut down (2-15 March). This result shows that the sources of these water inrush points were not due to the underground mining activities of the glauber brine or the rupture of the S02 well, but because of the brine leakage from other trona wells.

4.1.3. Components and mixed proportions of the inrush water

The PHREEQC simulation conditions were assumed to be as follows: (1) the trona brine did not mix with shallow groundwater after flowing through the mineral layer; or (2) the trona brine mixed with shallow groundwater in a ratio of 1:2, 1:10, 1:100, 1:200, 1:500, 1:1000 and 1:5000 after flowing through the mineral layer. The simulation results are shown in Table 3.

Table 3 shows that when the trona brine flowed through the stratum and shallow groundwater, the concentrations of Na^+, Cl^- and SO_4^{2-} decreased while the concentration of HCO_3^- increased with increasing proportion of the shallow water. The concentration of Ca^{2+} decreased at first and then increased.

The ion concentrations at Y-5, except for SO_4^{2-}, were similar to the ion concentrations in the trona brine. However, at the same time, the concentration of HCO_3^- was nearly 0. When the trona brine flowed through the layer, it would react rapidly and pour out of the ground directly because of the fast velocity of the inrush water at Y-5. Meanwhile, the trona brine was not continuously provided in the simulation. Thus, the concentration of HCO_3^- would be near to the concentration of trona brine in reality. Therefore, the trona brine must have a rapid inrush, nearly not mixing with shallow groundwater.

The PHREEQC simulation analysis results show that 1) the water inrush source of Y-5 was nearly all of the trona brine from the ruptured S02 well; 2) the water inrush source of Y-3 was a mixture of trona brine and groundwater in a ratio of from 1:10~1:100; and 3) the water inrush sources of Y-4, Y-2 and Y-1 were a mixture of trona brine and groundwater under the ratio of 1:200.

4.2. The channel of the inrush water

4.2.1. Reason for the brine leakage

Trona is produced by either a single well or double/multiple well convection mining method, a water-soluble mining method (Lin, 1987). The main mining unit consists of a salt cavity and production well. Thus, the instability of the salt cavity and the rupture of the production well are the main possible reasons for brine leakage.

(1) Analysis of salt cavity stability

The possibility of salt cavity collapse: Trona is distributed at the bottom of the second member of the Hetaoyuan Formation and in the upper part of the first member of the Hetaoyuan Formation, with dolomite strata developed in the roof and floor. The thick and hard surrounding rock structure determined that the cavity produce by hydrofracture but it is hard to fill with large-scale fractured channels and can remain intact and stable.

The development of a roof fracture: When a mineral is under exploitation, the surrounding rock in the cavity is under pressure from the inner brine. This pressure is equal to the water injection pressure plus the water column pressure in the production well. The water injection pressure of the trona production well is approximately 10-20 MPa, while the 1560.92-2929.53 m (mineral buried depth) water column pressure is approximately 15.3-28.71 MPa. Thus, the greatest water pressure on the surrounding rock in the cavity is 48.71 MPa. The main lithology of the surrounding rock is dolomite which is 500 m in thickness and 142.66 MPa in compressive strength, which is nearly 3 times that of the greatest possible water pressure. Therefore, large-scale fractures in the surrounding rock of the trona mineral would be difficult to develop under the effect of sustained water pressure.

(2) Analysis of production well rupture

The phenomenon of brine leakage caused by the S02 well rupture in Anpeng indicates that production well damage is an important cause of brine leakage. The depth of the S02 well rupture is 234 m underground, i.e. in the gypsum deposit, which is strongly hygroscopic. The pressure caused by the water swelling is approximately 0.15 MPa (Li and Zhou, 1996), which may damage the production well and induce brine leakage. The high concentration of SO_4^{2-} (>250 mg/L) generated by the reaction of leakage brine and gypsum can also corrode the production well and lead to groundwater inrush.

4.2.2. Analysis of water-conducting channel

According to our analysis, the most probable reason for brine leakage in trona is production well rupture. The leaking brine will flow along the water-conducting channel into the shallow aquifer and even pour out of the ground. However, the geological structure in the mining area shows no water-conducting fault development. Thus, the water-conducting channel, that the leakage brine flows along, is probably a fissure or artificial channel.

A structural fissure is the main type of fissure that occurs in groundwater inrush hazards when using the solution mining method. The structural fissure is determined by the maximum horizontal principal stress, which is controlled by the tectonic stress field in the mining area. The connection direction of the S02 well and the other water inrush points is NW-SE, which is the same as that of the structural fissure zone development direction. This indicates that the main water-conducting channel in Anpeng is controlled by the structural fissure zone.

The inrush points in Anpeng are all at the abandoned gypsum exploitation wells, which were not closed properly. Thus, high-pressure cavity water or leakage brine can flow along the structural fissure zone, finally connect with these wells, and then pour out of the ground through boreholes. Therefore, the abandoned gypsum exploitation wells are the main channels through which the shallow polluted groundwater flowed out of the ground, as shown in Fig. 5.

5. Conclusions

This study aimed to investigate the source and channel of the inrush water in a multilayer rock salt mining area. To achieve the set objectives, this study combined an analysis of geological and hydrogeological conditions, an analysis of physical and chemical reaction principles of different brines, the PHREEQC simulation method, and an analysis of geological and artificial reasons for the conducting channel where leakage brine flowed from the damage depth out to the ground as the study methodology.

Long-term solution mining with high-pressure and -temperature water not only dissolves minerals but also may cause rupture of strata and damage of the production well, which usually results in brine leakage or the inrush of groundwater. Geological and hydrogeological conditions are the basis which determines the total risk of the groundwater inrush hazard. Physical and chemical reaction principle analysis of different brines and hydrogeochemical simulation of water-rock interaction in different assumed conditions using the PHREEQC simulation method can not only determine the exact source of the leakage brine but also identify the mixed proportion of inrush water while the leakage brine flows through the mineral layer in different way. Other than geological reasons, mining techniques such as pressure control of injection water and groundwater quality monitoring of exploitation wells may also determine the risk of a groundwater inrush hazard in a multilayer rock salt mining area.

Acknowledgements

This work was partially supported by the Fundamental Research Funds for the Central Universities, China University of Geosciences (Wuhan) [Grant Numbers: CUGL100219].

Author Contributions

Bin Zeng and Tingting Shi contributed to data analysis and manuscript writing; Zhihua Chen proposed the main structure of this study; Liu Xiang and Muyi Yang designed and performed the experiments; and Shaopeng Xiang performed the PHREEQC simulation. All the authors read and approved the final manuscript.

Conflicts of Interest

The authors declare that they have no conflict of interest.

References

Blachowski, J., Milczarek, W. and Stefaniak, P.: Deformation information system for facilitating studies of mining-ground deformations, development, and applications, Nat. Hazards Earth Syst. Sci., 14, 1677-1689, 2014

Bonetto, S., Fiorucci, A., Fornaro, M. and Vigna, B.: Subsidence hazards connected to quarrying activities in a karst area: the case of the Moncalvo sinkhole event (Piedmont, NW Italy), Estonian J. Earth Sci., 57, 125-134, 2008

Chen, H. J. and Li, X. Bi.: Studies of water source determination method of mine water inrush based on Bayes' multi-group stepwise discriminant analysis theory, Rock and Soil Mechanics., 30, 3655-3659, 2009.

Clark, I. D. and Fritz, P.: Environmental isotopes in hydrogeology, Lewis Publishers, New York, USA, 35-37, 1997.

Closson, D. and Abou Karaki, N.: Salt karst and tectonics: sinkholes development along tension cracks between parallel strike-slip faults , Dead Sea , Jordan. Earth Surface Processes and Landforms., 1408-1421, 2009

Cobbina, S.J., Duwiejuah, A.B., Quansah, R., Obiri, S. and Bakobie, Noel.: Comparative Assessment of Heavy Metals in Drinking Water Sources in Two Small-Scale Mining Communities in Northern Ghana, Int. J. Environ. Res. Public Health., 12, 10620-10634, 2015.

Ezersky, M., Legchenko, A., Camerlynck, C. and Al-Zoubi, A.: Identification of sinkhole development mechanism based on a combined geophysical study in Nahal Hever South area (Dead Sea coast of Israel). Environmental Geology., 58, 1123-1141, 2009

Ezersky, M. and Frumkin, A.: Fault - Dissolution front relations and the Dead Sea sinkhole problem. Geomorphology., 201, 35-44, 2013

Fernandez, I., Olias, M., Ceron, J.C. and De la Rosa, J.: Application of lead stable isotopes to the Guadiamar Aquifer study after the mine tailings spill in Aznalcollar (SW Spain), Environ Geol., 47, 197-204, 2005.

Fernandez-Galvez, J., Barahona, E., Iriarte, A. and Mingorance, M.D.: A simple methodology for the evaluation of groundwater pollution risks, Sci Total Environ**.,** 378, 67-70, 2007.

Frumkin, A., Ezersky, M., Al-Zoubi, A., Akkawi, E. and Abueladas, A.-R.: The Dead Sea sinkhole hazard: Geophysical assessment of salt dissolution and collapse. Geomorphology., 134, 102-117, 2011

Goldscheider, N. and Bechtel, T.D.: The housing crises from underground – damage to a historic town by geothermal drillings through anhydrite, Staufen, Germany. Hydrogeology Journal., 17, 491-493, 2009

Gao, W.D.: Application of Entropy Fuzzy Discriminating methods in Distinguishing Mine

Bursting Water Source, Mining Safety & Environmental Protection., 39, 22-24, 2012.

Gutierrez, F., Parise, M., De, Waele, J. and Jourde, H.: A review on natural and human-induced geohazards and impacts in karst. Earth Science Reviews., 138, 61-88, 2014

Hao, B.B., Li C. and Wang C.H.: Application of grey correlation degree in the identification of sources of mine water bursting, China Coal., 36, 20-22, 2010.

Hu, W.W., Ma, Z.Y., Cao, H.D., Liu, F., Li, T. and Dou, H.P.: Application of Isotope and Hydrogeochemical Methods in Distinguishing Mine Bursting Water Source, Journal of Earth Sciences and Environment., 32, 268-271, 2010.

Houben, G.J., Sitnikova, M.A. and Post, V.E.A.: Terrestrial sedimentary pyrites as a potential source of trace metal release to groundwater – A case study from the Emsland, Germany, Appl. Geochem., 76, 99-111, 2017.

Jiang, R.Z. and Jiang T.X.: Present Development and Prospecting of Hydraulic Fracturing Technology, Oil Drilling & Production Technology., 26, 52-57, 2004.

Kang, X.B., Hu, X.W. and Xie, H.Q.: Numerical simulation on the influence of the groundwater flow field during tunneling, Advanced Materials Research., pp. 1230-1233, 2012.

Kotwica, K.: Scenarios of technological development of roadwavs mining in polish coal mines conditions, Gospod Surowcami Min., 24, 139-152, 2008.

Lee, H., Choi, Y., Suh, J. and Lee, S.H.: Mapping Copper and Lead Concentrations at Abandoned

Mine Areas Using Element Analysis Data from ICP–AES and Portable XRF Instruments: A Comparative Study, Int. J. Environ. Res. Public Health., 13, 384, 2016.

LeDoux, T.M., Szynkiewicz, A. and Faiia, A.M.: Chemical and isotope compositions of shallowgroundwater in areas impacted by hydraulic fracturing and surface mining in the Central Appalachian Basin, Eastern United States, Appl. Geochem., 71, 73-85, 2016.

Lin, Y.X.: The History of Science & Technology of well salt in China, Sichuan Science and Technology Pres, Chengdu, 1987.

Li, D.D. and Zhou, Z.A.: Possibility of corrosion failure of concrete shaftwall due to water infiltration, Journal of China Coal Society., 21, 158-163, 1996.

Liu, H., Yang, T., Zhu, W. and Yu, Q.: Numerical analysis of the process of water inrush from the 12th coal floor FANGEZHUANG coal mine in China, Controlling Seismic Hazard and Sustainable Development of Deep Mines: 7th International Symposium on ROCKBURST and Seismicity in Mines (RASIM7)., 1&2, 1381-1386, 2009.

Liu, R.Z., Liu, J., Zhang, Z.J., Borthwick, A. and Zhang, K.: Accidental Water Pollution Risk Analysis of Mine Tailings Ponds in Guanting Reservoir Watershed, Zhangjiakou City, China, Int. J. Environ. Res. Public Health., 12, 15269-15284, 2015.

Lollino, P., Martimucci, V. and Parise, M.: Geological survey and numerical modeling of the potential failure mechanisms of underground caves. Geosystem Engineering., 16, 100-112, 2013

Lu, J.T.: Recognizing of Mine Water Inrush Sources Based on Principal Components Analysis and Fisher Discrimination Analysis Method, China Safety Science Journal., 22, 109-115, 2012.

Ma, L. and Qian, J.Z.: An approach for quickly identifying water-inrush source of mine based on GIS and groundwater chemistry and temperature, Coal Geology & Exploration., 42, 49-53, 2014.

Namin, F. S., Shahriar K., Bascetin A. and Ghodsypour S.H.: Practical applications from decision-making techniques for selection of suitable mining method in Iran, Gospod Surowcami Min., 25, 57-77, 2009.

Parise, M., and Gunn, J.: Natural and anthropogenic hazards in karst areas: Recognition, Analysis and Mitigation. Geol. Soc. London, sp. publ. 279, 2007

Parise, M. and Lollino, P.: A preliminary analysis of failure mechanisms in karst and man-made underground caves in Southern Italy. Geomorphology., 134, 132-143, 2011

Parise, M., Closson, D., Gutierrez, F. and Stevanovic, Z.: Anticipating and managing engineering problems in the complex karst environment. Environmental Earth Sciences., 74, 7823-7835, DOI :10.1007/s12665-015-4647-5, 2015

Qiu, Z.Y.: Mechanism analysis of surface collapse in the area of solution salt mining, Journal of

Safety Science and Technology., 7, 27-31, 2011.

Ramadas, M., Ojha, R. and Govindaraju, R.S.: Current and Future Challenges in Groundwater. II: Water Quality Modeling, J. Hydrol. Eng., 13, 132-140, 2015.

Robins, N.S.: Groundwater quality in Scotland: major ion chemistry of the key groundwater bodies, Sci Total Environ., 294, 41-56, 2002.

Shao, A.J., Huang, Y. and Meng, Q.X.: Numerical Simulation on Water Invasion of Coal Mine, Applied Mechanics and Materials., pp. 1112-1117, 2013.

Shi, T.T., Chen, Z.H. and Luo, Z.H.: Mechanism of groundwater bursting in a deep rock salt mine region: a case study of the Anpeng trona and glauber salt mines, China, Environ Earth Sci., 68, 229-239, 2013.

Staudtmeister, K. and Rokahr, R.B.: Rock Mechanical Design of Storage Caverns For Natural Gas in Rock Salt Mass, Rock Mech&Min.Sci., 34, 3-4, 1997.

Vigna, B., Fiorucci, A., Banzato, C., Forti, P. and De Waele, J.: Hypogene gypsum karst and sinkhole formation at Moncalvo (Asti, Italy). Z. Geomorphol., 54, 285-308, 2010

Wang, J.M.: A Preliminary Study on the Characteristics and Conditions of forming Anpeng Trona deposits, Petrol Explor Dev., 5, 93-99, 1987.

Waltham, AC. And Fookes, PG.: Engineering classification of karst ground conditions. Quarterly Journal of Engineering Geology and Hydrogeology., 36, 101-118, 2003

Wei, Y.N.: Research and Application of Hydro-geochemical Simulation, Journal of Water Resources and Water Engineering., 21, 58-61, 2010.

Wu, Q., Li, B. and Chen, Y.: Vulnerability Assessment of Groundwater Inrush from Underlying Aquifers Based on Variable Weight Model and its Application, Water Resour Manag., 30, 3331-3345, 2016.

Xu, H. and Li, H.S.: Study on $CaSO_4$ crystallization process and its influential factors, Industrial Water Treatment., 5, 67-69, 2011.

Yang, Y.H.: Gypsum mineral dissolution kinetics, M.D. thesis, China University of Geosciences, Wuhan, China, 2003.

Yuan, W.H. and Gui, H.R.: The Characteristics of Geothermal Temperature and Its Application in Distinguishing the Source of Water in Ren Lou Mine, Journal of Anhui University of Science and Technology (Natural Science)., 25, 9-11, 2005.

Zhou, W. and Beck, BF.: Engineering issues on karst. In: P. van Beynen (Ed), Karst Management. Springer, Dordrecht, pp. 9-45, 2011

Figure captions

Fig. 1. One of the long-term (longer than 2 years) groundwater inrush points with stable discharge (Y-3).

Fig. 2. The sudden groundwater inrush point (Y-5). As shown in this figure, the high-temperature inrush groundwater was being pumped after the ground was broken.

Fig. 3. Information about strata, lithology, aquifers, and buried positions of each ore bed in the mining area.

Fig. 4. Sketch map of hydrogeological conditions and the distribution of groundwater inrush points in the mining area.

Fig. 5. Schematic diagram of source and channel analysis of the groundwater inrush hazard in the multilayered rock salt mining area in Tongbai County.

Fig.1

Fig.2

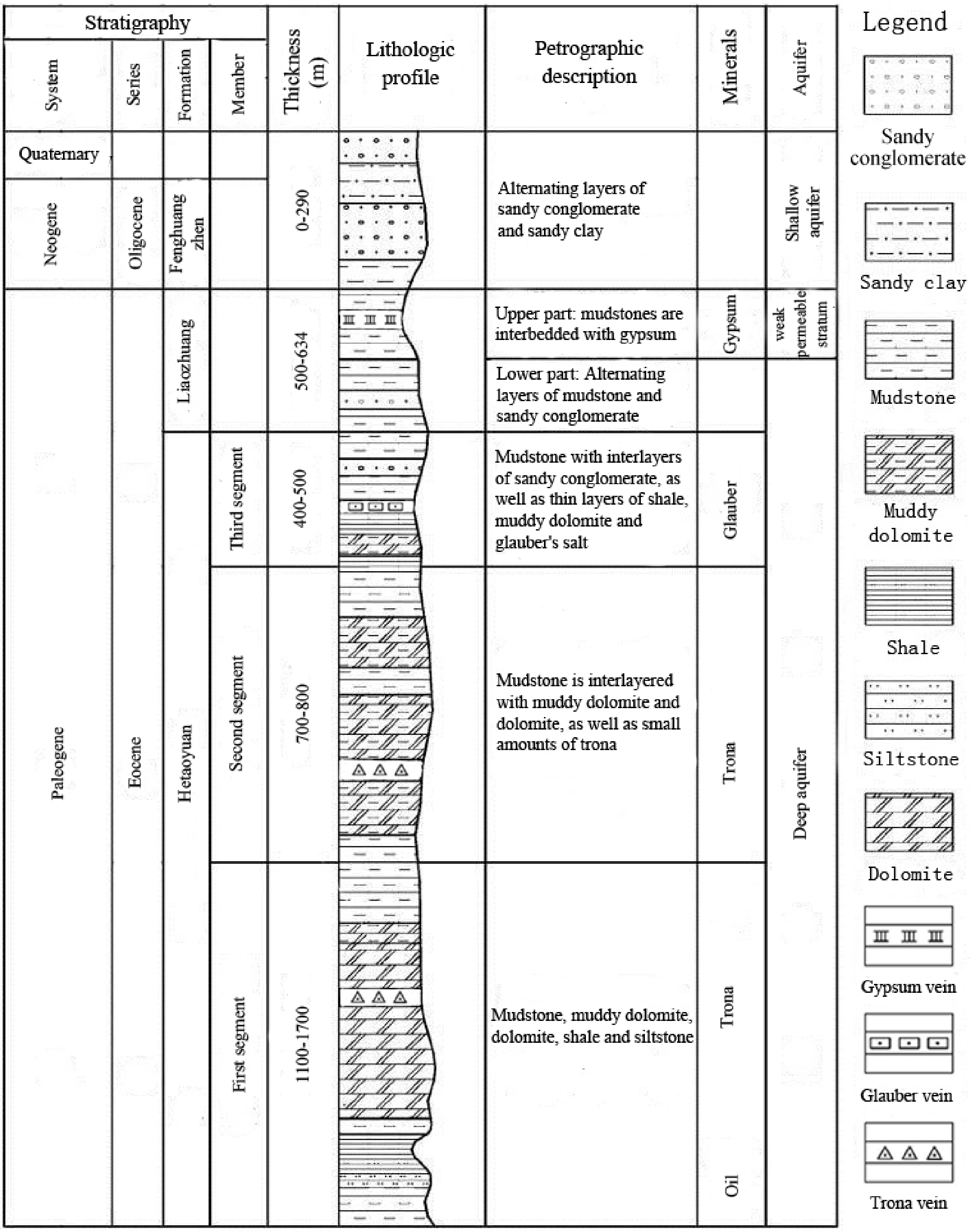
Stratigraphy
System
Series
Formation
Member
Thickness (m)
Lithologic profile
Petrographic description
Minerals
Aquifer
Legend
Quaternary
Neogene
Oligocene
Fenghuang zhen
0-290
Alternating layers of sandy conglomerate and sandy clay
Shallow aquifer
Paleogene
Eocene
Liaozhuang
500-634
Upper part: mudstones are interbedded with gypsum
Gypsum
weak permeable stratum
Lower part: Alternating layers of mudstone and sandy conglomerate
Hetaoyuan
Third segment
400-500
Mudstone with interlayers of sandy conglomerate, as well as thin layers of shale, muddy dolomite and glauber's salt
Glauber
Second segment
700-800
Mudstone is interlayered with muddy dolomite and dolomite, as well as small amounts of trona
Trona
Deep aquifer
First segment
1100-1700
Mudstone, muddy dolomite, dolomite, shale and siltstone
Trona
Oil
Sandy conglomerate
Sandy clay
Mudstone
Muddy dolomite
Shale
Siltstone
Dolomite
Gypsum vein
Glauber vein
Trona vein

Fig.3

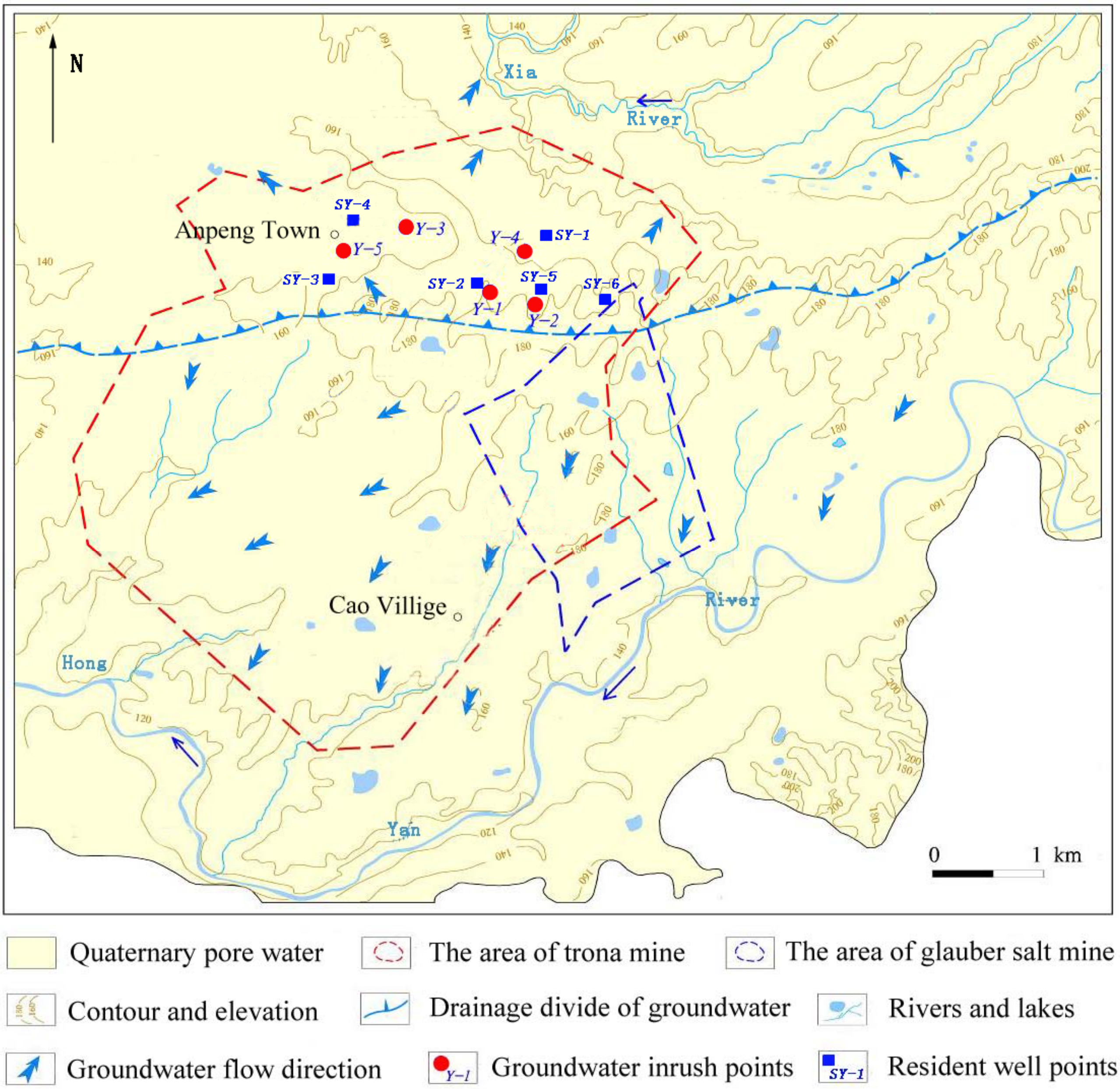
N
Xia
River
Anpeng Town
SY-4
Y-3
Y-5
Y-4
SY-1
SY-3
SY-2
SY-5
SY-6
Y-1
Y-2
Cao Villige
River
Hong
Yan
0
1 km
Quaternary pore water
The area of trona mine
The area of glauber salt mine
Contour and elevation
Drainage divide of groundwater
Rivers and lakes
Groundwater flow direction
Groundwater inrush points
Resident well points

Fig.4

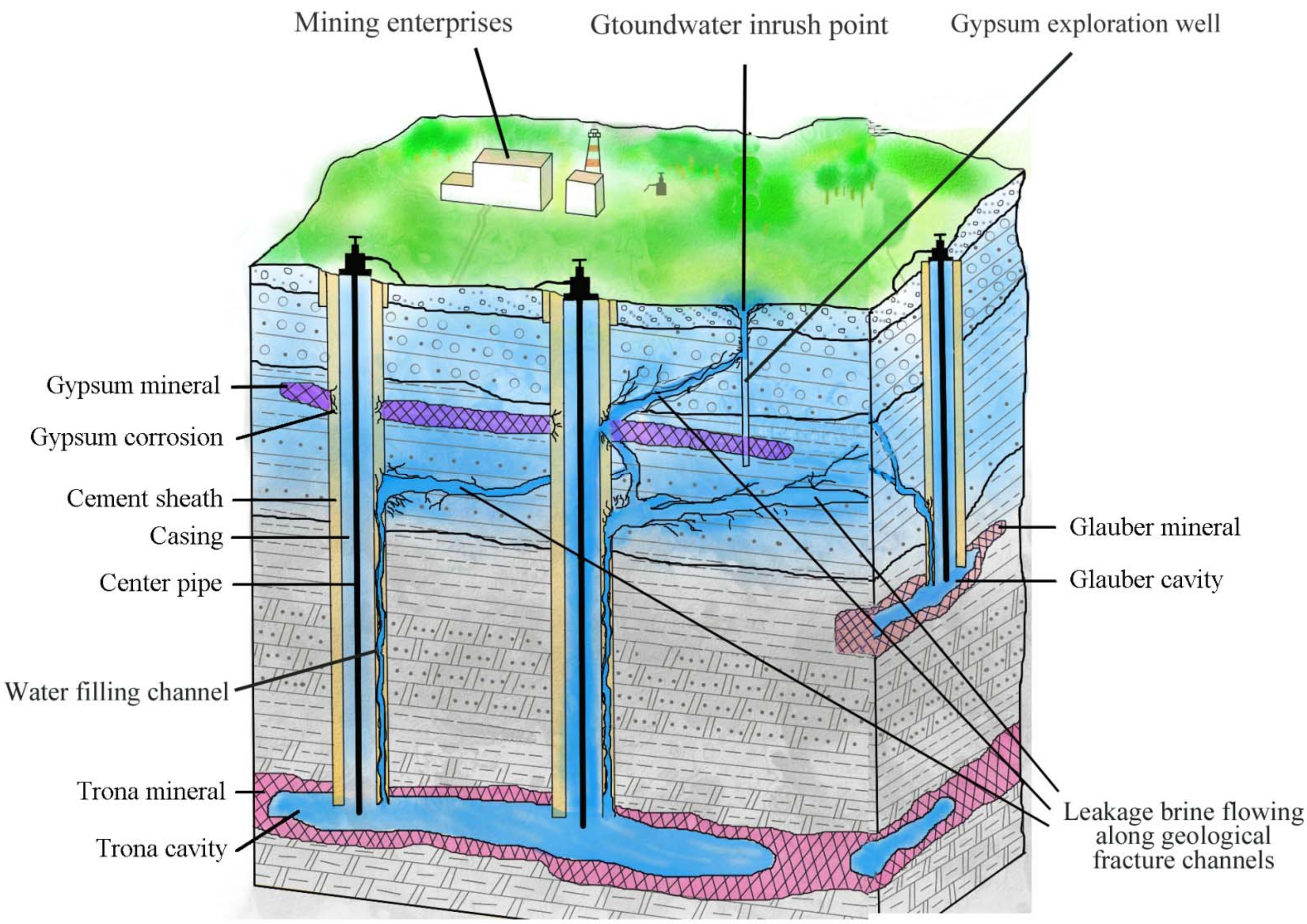
Mining enterprises
Gtoundwater inrush point
Gypsum exploration well
Gypsum mineral
Gypsum corrosion
Cement sheath
Casing
Center pipe
Water filling channel
Trona mineral
Trona cavity
Glauber mineral
Glauber cavity
Leakage brine flowing
along geological
fracture channels

Fig.5

Table 1 Initial data of trona brine and background value of groundwater for the PHREEQC simulation

Type	Temperature (° C)	pH	Na^{+}	Ca^{2+}	Mg^{2+}	Cl^{-} (mg/L)	SO_4^{2-}	HCO_3^{-}	CO_3^{2-}
Trona brine	70.0	10.8	85880	5.0	1.0	3819	206.0	104721	4565
Background value of groundwater	14.1	7.5	38.76	67.10	23.88	12.46	39.31	386.87	0.00

Table 2 Chemical composition of groundwater from the inrush hazard points and surrounding resident wells

Source	Point	Na^+ (mg/L)	Ca^{2+} (mg/L)	Mg^{2+} (mg/L)	Cl^- (mg/L)	SO_4^{2-} (mg/L)	HCO_3^- (mg/L)	CO_3^{2-} (mg/L)	Salinity (mg/L)	Depth (m)
Groundwater from inrush hazard points	Y-1	447.30	91.2	74.68	171.18	278.55	1488.89	0.00	1807.35	330.55 ~ 430.2
	Y-2	524.50	89.34	75.32	153.97	298.88	1525.00	0.00	1904.51	
	Y-3	1132.00	146.6	158.30	125.56	4296.44	1012.93	0.00	6365.37	
	Y-4	322.12	98.67	123.88	210.78	346.55	1122.77	0.00	1663.38	
	Y-5	50300.00	12.23	53.21	3813.80	12858.63	81309.15	27159.0	107692.4	
Groundwater from resident wells around the inrush points	SY-1	46.28	76.76	17.29	64.3	14.58	319.03	0.00	378.73	10.00
	SY-2	28.37	98.02	27.46	26.16	10.38	453.84	0.00	417.31	
	SY-3	43.14	46.2	14.42	31.02	117.12	319.03	0.00	316.26	
	SY-4	118.53	278.4	72.3	425.23	175.96	568.52	0.00	1354.68	
	SY-5	31.67	95.51	19.22	53.93	22.59	351.97	0.00	398.9	
	SY-6	36.77	68.82	19.6	18.51	21.55	340.38	0.00	335.43	

Table 3 Simulation results for a mixed proportion of inrush trona brine using the PHREEQC method (mg/L)

Conditions	Mixed proportion with shallow groundwater	Na^+	Ca^{2+}	Cl^-	SO_4^{2-}	HCO_3^-
Trona brine unmixed or mixed with different proportion of shallow groundwater after flowing through the mineral layer (simulation results)	Unmixing	87147.00	301.08	3880.15	68659.20	5.06
	1:1	48093.00	280.00	2145.62	37900.80	9.39
	1:2	33235.00	184.72	1485.68	26188.80	13.97
	1:10	9586.40	148.28	436.30	7561.92	57.95
	1:100	1098.25	90.40	141.63	873.89	306.34
	1:200	571.78	69.60	118.56	459.17	382.17
	1:500	252.77	68.32	104.60	207.84	453.66
	1:1000	144.81	67.52	99.94	105.12	481.60
Water quality test results in five water inrush hazard points	Y-1	447.30	91.20	171.18	276.55	1488.89
	Y-2	524.50	89.34	153.97	298.88	1525.00
	Y-3	1132.00	146.60	125.56	4296.44	1012.93
	Y-4	322.12	98.67	210.78	346.55	1122.77
	Y-5	50300.00	12.23	3813.80	12858.63	81309.15